

Supporting Information

Stan et al. 10.1073/pnas.0914233107

SI Methods

Cell Culture and Transfection. Proliferating mouse ES cells inheriting an N-cadherin deletion (1, 2) in homozygous (*Ncad*^{-/-}) or in heterozygous (*Ncad*^{+/-}) configuration were cultured on mitomycin C-inactivated mouse embryonic feeder cells in the presence of leukemia inhibitory factor (LIF). In vitro differentiation was done using an embryoid body (EB) system. Briefly, EB formation occurred in hanging drop culture without LIF and in the presence of retinoic acid (for further details, see refs. 3 and 4). Purification of ES cell-derived neurons was performed by using the L1 immunoisolation technique as described (3, 4). In brief, a plastic Petri dish was coated overnight with goat anti-rat IgG and then with supernatant from a rat anti-L1 antibody-producing hybridoma cell line. For L1 immunoisolation, EBs were dissociated mechanically after papain treatment. The cell suspension was added to the L1-coated Petri dish, and after 1.5 h at room temperature, the non-adherent cells were washed away. The adherent cells were harvested from the Petri dish and were resuspended in PBS/25% FBS. Cortical neurons were used in addition to ES cell-derived neurons to ensure that similar effects are observed in neurons differentiated in vivo. Cortical neurons were prepared from E17 C57BL/6 mice as described (5). Purified ES cell-derived neurons or cortical neurons were cultured on a confluent monolayer of glial cells, resulting in the formation of both autapses and synapses. Glial cells were obtained by dissociating the cortex of C57BL/6 mice at postnatal day 0–2 and culturing proliferating cells for several weeks in serum-containing medium. Confluent glial cells completely devoid of neurons were dissociated and were seeded on uncoated glass bottom dishes in BME⁺ medium and cultured 4–6 d in the presence of cytosine- β -D-arabinofuranoside (10 μ M) to inhibit proliferation. ES cell-derived, L1-selected neurons or cortical neurons were seeded on glial cells at a density of 5×10^5 cells per 35 mm² dish and were cultured in Neurobasal medium with the addition of B27 supplement, glutamax, and penicillin/streptomycin. DNA transfection was performed by using Lipofectamine 2000 (Invitrogen), following the manufacturer's instructions. Two days after transfection, successfully transfected neurons were detected by EGFP and DsRed2 fluorescence.

Generation of shRNA Constructs and Recombinant Lentiviruses, and Infection of Cultured Cortical Neurons. For performing RNA interference-mediated knockdown of S-SCAM/MAGI-2, the hairpin sequences used were as follows:

sh-KD (knockdown): GCCAGTCTATCATCAACATGCGT-GAAGCCACAGATGGCATGTTGATGATAGACTGGC.

sh-MM (mismatch): GCTAGTCTAGCATCATCATGCGT-GAAGCCACAGATGGCATGATGATGCTAGACTAGC.

Annealed synthetic oligonucleotides were ligated into FUGW (6) under control of the U6 promoter. The vector carries EGFP under control of the Ubiquitin promoter and, therefore, marks all shRNA-expressing cells. Recombinant lentiviruses for delivery of expression plasmids were generated as described (7). Briefly, HEK293T cells were cotransfected with FUGW and plasmids encoding the vesicular stomatitis virus glycoproteins VSVg, gag, and pol by using Lipofectamine 2000 (Invitrogen). Viruses were harvested from the culture medium 2 d after transfection and were concentrated by centrifugation. For each viral preparation, titers were estimated by infecting cultured cortical neurons.

Cortical neurons from E17 mice were cultured at low density using standard protocols (8). At 2 DIV, neurons were infected

with lentiviruses delivering either control mismatch shRNAs or knockdown shRNAs directed against S-SCAM/MAGI-2 α , β , and γ . To confirm that the used constructs reduced the expression of S-SCAM/MAGI-2 proteins, total cell lysates were collected from infected (mismatch control and knockdown) and not infected cultures (control) at 8 DIV. Western blotting revealed a strong reduction in S-SCAM/MAGI-2 proteins in knockdown condition, whereas no changes were observed with the mismatch control (Fig. S9). Antibodies used for Western were rabbit anti-MAGI-2 (Sigma) and mouse anti-tubulin (Sigma).

Organotypic Slice Culture and Single-Cell Electroporation. Organotypic hippocampal slice cultures were prepared from 1-d-old Wistar rats according to the Stoppini method. Brains were rapidly removed, and 375-mm-thick sagittal slices were cut by using a tissue chopper (McIlwain). The hippocampal formation, subicular, and entorhinal cortex were isolated from the slice. The hippocampi were maintained in cold (4 °C) minimum essential medium (MEM) supplemented with glutamine and placed on top of polytetrafluoroethylene membranes (Millicell-CM; Millipore) with 1.0 mL of culture medium consisting of Neurobasal (NB) medium supplemented with 2% B27 (Invitrogen), containing 1% FCS and 5 mM MgCl₂, 25 U/mL penicillin, and 25 μ g/mL streptomycin. The slices were kept in an incubator with 5% CO₂ at 37 °C, and the medium was changed every third day. AraC (10 μ M) was added to the medium every fifth day.

Single-cell electroporation was performed in these hippocampal slice cultures at 5 DIV with an ELC-03M loose-patch amplifier (NPI instruments) by using infrared differential interference contrast optics (IR-DIC) video microscopy. CA3 pyramidal cells were selected based on morphological criteria. Electroporation pipettes were filled with DNA solution dissolved in extracellular solution (concentration of DNA: 0.33 μ g/ μ l). The extracellular solution consisted of 110 mM NaCl, 5 mM KCl, 1 mM MgCl₂, 2 mM CaCl₂, 15 mM HEPES, 0.01 mM glycine, and 10 mM glucose. After reaching the cell attached mode, the cell was stimulated with high-frequency pulses of 1.5 V amplitude. The slices were returned into the incubator and were fixed 2 d after transfection.

Immunocytochemistry. For immunocytochemistry, ES cell-derived neurons or cortical neurons were cultured on poly-L-ornithine-coated glass coverslips without added glia. To ensure sufficient supply with glia-derived factors, the glass coverslips were placed on a monolayer of cultured glial cells. Neurons were fixed with PBS containing 4% paraformaldehyde for 20 min, washed three times with PBS and incubated for 30 min at room temperature in buffer 1 (10% FCS, 5% sucrose, 2% BSA, and 0.3% Triton X-100 in PBS). Cells were then incubated for 1 h at room temperature with the first antibody in buffer 1, washed with PBS, and incubated overnight at 4 °C with the secondary antibody in buffer 2 (buffer 1 without FCS). The cells were rinsed again with PBS and imaged immediately.

Rat hippocampal slice cultures were fixed 2 d after electroporation with PBS containing 4% paraformaldehyde for 3 h, washed three times with PBS, and incubated for 1 h at room temperature in buffer 1. Then the slices were incubated overnight at room temperature with the first antibody in buffer 1, washed with PBS, and incubated for 2 h at room temperature with secondary antibody in buffer 2. Slices were mounted with a glass coverslip on a microscope slide by using AquaPoly/Mount (Polysciences).

Primary antibodies used in this study included rabbit polyclonal anti-GFP (Abcam); mouse monoclonal anti-VAMP2 (Syn-

aptic Systems), rabbit polyclonal anti-VAMP2 (Synaptic Systems), mouse monoclonal anti-bassoon (Assay Designs), chicken polyclonal anti-MAP2 (Abcam), mouse monoclonal anti-panneurologin (Synaptic Systems), rabbit polyclonal anti-PSD95 (Zymed/Invitrogen); and rabbit polyclonal anti-N-cadherin (Abcam). Secondary antibodies included Cy3 IgG goat anti-mouse (Chemicon), FITC IgY goat anti-chicken (Abcam), Oregon green 488 IgG goat anti-rabbit (Molecular Probes), Alexa Fluor 488 goat anti-rabbit, and Alexa Fluor 546 goat anti-mouse (Invitrogen). For quantitative analysis, the proximal parts ($\leq 50 \mu\text{m}$ from the soma) of the main dendrites were selected. Dendritic segments with a minimum length of $15 \mu\text{m}$ were used.

Fluorescence Imaging. Z stacks of fluorescence images (10–15 planes at $1 \mu\text{m}$ depth) were acquired from cultured neurons by using a computer-controlled Zeiss Axiovert 200M inverted microscope equipped with a piezoelectric focus drive, thus enabling 3D deconvolution of the obtained images. Image acquisition was done with a 12-bit monochrome CoolSNAP ES CCD camera (Photometrics) by using MetaView software (Visitron Systems). All images were captured with the same exposure time (0.2 s per frame). Images were binned 2×2 to minimize photobleaching and photodamage to live cells.

For live-cell imaging of neurons expressing fluorescent proteins, neurons were cultured on a glia monolayer in glass-bottom dishes (Willco Wells). For time-lapse imaging, cells in their culture medium were imaged on the Zeiss Axiovert 200M deconvolution microscope equipped with a temperature controlled and CO_2 controlled small incubator (CTI-controller 3700 digital and Temp-control 37-2 digital, Zeiss). Cells were kept at constant temperature (37°C), CO_2 atmosphere (5%) and humidity. The cells were allowed to equilibrate for a period of at least 30 min before they were subjected to time lapse imaging. Images were obtained every 20 min by using a $\times 63$ oil immersion objective (Plan-Apochromat $\times 63/1.40$ Oil DIC; Zeiss). The objective was equipped with an objective heater kept at 37°C to eliminate any thermal gradient between objective and specimen. To correct for out-of-focus fluorescence in the field of view, z-stacked images at $1 \mu\text{m}$ depth (10–15 planes) were acquired at each time interval by using a piezoelectric focus drive. Two sets of z stacks for EGFP and DsRed2 signal were collected automatically at every time point by using a time-lapse journal written in MetaMorph software to control the filter wheel (equipped with filter set 17 for EGFP and filter set 43 for DsRed2; Zeiss) and the shutter (exposure time 0.2 s per frame). Images were acquired with a binning of 2×2 for both signals. With these settings, the cluster dynamics could be observed for a time period of 2 h without any significant photobleaching.

Fixed hippocampal slice cultures were imaged with a Zeiss LSM 510 confocal microscope. Neurons expressing EGFP were visualized by using the 488-nm Argon laser line, whereas the VAMP2 signal was visualized by using the 543-nm He/Ne laser line. To image VAMP2 puncta a $\times 63$ oil immersion objective (Plan-Apochromat $\times 63/1.40$ Oil DIC; Zeiss) was used with an additional electronic zoom factor of 4. To visualize dendritic segments at different focal planes, z-stacked images (20–30 optical sections) at $1\text{-}\mu\text{m}$ -depth intervals were acquired by using the LSM 510 software. Laser illumination was attenuated to 25% of the laser power and the detector pinhole was opened to improve light collection. The detector gain was adjusted to permit detection of weak diffuse fluorescence signal as well as intensely fluorescent clusters.

Three-Dimensional Deconvolution, Digital Image Processing, and Quantitative Analysis. Z stacks of fluorescence images acquired with MetaView software were imported in the AutoDeblur software (Visitron Systems) and were subjected to 3D deconvolution, using the blind deconvolution algorithm. In this algorithm, the point spread function (PSF) is considered unknown and is estimated only by the optics in use and from the information within

the dataset. Using the maximum-brightness operation in MetaMorph software, the deconvolved image stacks were projected along the z axis, creating an output image each of whose pixels contains the maximum value over all images in the stack at the particular pixel location.

For analysis of VAMP2 and Bassoon puncta, images were thresholded offline by applying the autothreshold function of MetaMorph software. The autothreshold function uses the histogram data to determine the optimum threshold value for the image. The autothreshold assumes that there is a peak at the background intensity level, which has a width based on noise or other image variations. A three-tier approach is taken for each image. First, the largest peak is found and assumed to be the background. A search is done for the local minimum. The minimum is assumed to be the trough between the background and the object intensity level. If the local minimum is found, then the number of pixels selected by the threshold is calculated. If no local minimum was found, or if $<1\%$ of the pixels are above the threshold, then it is assumed that the major peak was actually the object data and the search is done for an earlier peak. If no early peak is found (one smooth curve), the code defaults to using the SD from the image as an estimate for noise. Pixels beyond two times SD from the peak are determined to be from object data. For the Autothreshold operation to perform better, the soma of the neurons was excluded from the image analysis. For this, regions located on the proximal dendrites were cut out from the original maximum image and the autothreshold function was applied. Because the neurologin and the PSD95 signals showed a diffuse dendritic distribution in addition to clusters, the autothreshold operation could not be used to discriminate the clusters. Therefore, the threshold value was manually set so that only a few individual pixels outside of the clusters remained above threshold.

After the threshold operation, a low pass filter operation was applied to remove individual pixels from the background noise left in the image. The Integrated morphometry analysis tool in MetaMorph software was used to perform automatic morphometric measurements of objects in the low pass images. Additionally, a classifier filter was defined, which restricted the measurements only to clusters bigger than 8 pixels in size. The data were logged in Microsoft Excel files and then imported in Sigma Plot for further analysis. For analyzing the colocalization of puncta, regions of interest (ROI) fitting to the clusters in the low pass images were calculated for the two different fluorescence signals. The operation defines ROIs that outline objects automatically by determining the edges of objects based on the thresholding overlay. If the ROIs corresponding to the two fluorescence signals were presenting overlapping pixels, then the objects were considered to be colocalized.

Detection of VAMP2 clusters on EGFP-expressing dendrites of electroporated neurons in hippocampal slice cultures was performed in a blind fashion by using the 4D Viewer module in MetaMorph software, which allowed simultaneously 3D isosurface visualization and rotation of objects in both wavelengths. For quantitative analysis, the proximal parts ($\leq 50 \mu\text{m}$ from the soma) of the main dendrites were selected. Dendritic segments with a minimum length of $15 \mu\text{m}$ were used.

For calculations and statistical analysis data were imported to Microsoft Excel and SigmaPlot 9.0 (Jandel Scientific). All data are given as mean \pm SEM. Statistical analysis was carried out with Student's *t* test or one-way ANOVA, respectively.

Fluorescence Recovery After Photobleaching. FRAP experiments were conducted with a Zeiss LSM 510 confocal microscope. Cultured ES cell-derived neurons expressing EGFP-synaptobrevin2 (VAMP2) were visualized by using the 488-nm Argon laser line and the fluorescein filter set. For FRAP experiments the neuronal cultures were kept in a Hepes-buffered extracellular solution (in: 130 mM NaCl, 5 mM KCl, 1 mM MgCl_2 , 2.5 mM CaCl_2 and

20 mM Hepes, pH 7.3). The chamber was maintained at constant temperature (37 °C). To image EGFP-VAMP2 puncta a $\times 63$ oil immersion objective was used with an additional electronic zoom factor of 2–4. To correct for out-of-focus fluorescence, z-stacked images (10–15 optical sections with a 512×512 pixel array) at 1- μ m depth intervals were collected every 5 min by using the LSM 510 software. Laser illumination was attenuated to 25% of the laser power, and the detector pinhole was opened (1.5 Airy disk) to improve light collection. The detector gain was adjusted to permit detection of weak diffuse EGFP fluorescence and intensely fluorescent clusters. Photobleaching was performed by defining an ROI around a single VAMP2 punctum, and then 150 frames were scanned within the selected area to effectively bleach fluorescent molecules in this region. FRAP data were normalized to the fluorescence intensity before photobleaching and corrected for ongoing photobleaching according to the following equation:

$$F_{\text{cor}t} = (F_t/F_0)/(F_{\text{nb}t}/F_{\text{nb}0}),$$

where F_t is the fluorescence intensity at time t , F_0 is the prephotobleaching fluorescence intensity, $F_{\text{nb}t}$ is the average fluorescence intensity of 2–4 nonbleached puncta at time t , and $F_{\text{nb}0}$ is the average fluorescence intensity of the same nonbleached puncta at time $t = 0$.

Electrophysiology. Whole-cell patch clamp recordings were obtained from transfected ES cell-derived neurons at 12–14 DIV, as described (3). The intracellular solution contained 110 mM KCl, 0.25 mM CaCl₂, 10 mM EGTA, 20 mM Hepes, pH 7.3. The extracellular solution contained: 130 mM NaCl, 5 mM KCl, 2.5

mM CaCl₂, 1 mM MgCl₂, 20 mM Hepes, pH 7.3. AMPA receptor-mediated miniature EPSCs were isolated by addition of 1 μ M TTX and 10 μ M gabazine and were recorded at a holding potential of -60 mV. AMPA mEPSCs were completely blocked after the addition of 20 μ M DNQX. Quantitative analysis of miniature EPSCs was performed by using the Mini Analysis software (Synaptosoft). Statistical analysis was done by using Student's t test.

For determining the kinetics of MK-801 (20 μ M) block, NMDA EPSCs were recorded from transfected mouse cortical neurons at 12–14 DIV. The intracellular solution was as above. The Mg²⁺-free extracellular solution contained 130 mM NaCl, 5 mM KCl, 2.5 mM CaCl₂, and 20 mM Hepes at pH 7.3 with glycine (10 μ M), gabazine (10 μ M), and DNQX (15 μ M) added. Holding potential was -70 mV. NMDA EPSCs were elicited by standard extracellular stimulation at 0.05 Hz. Peak amplitudes of NMDA EPSCs were analyzed by using PClamp9 software (Molecular Devices).

Recombinant DNA. Full-length mouse S-SCAM (amino acids 1–1112) (generous gift from M. G. Price and D. L. Burgess, Baylor College of Medicine, Houston, TX) was used as a template for PCR amplification of full-length S-SCAM, S-SCAM-PDZ1del (lacking amino acids 1–403), S-SCAM-PDZ5del (lacking amino acids 964–1112) by standard procedures. Amplified fragments were cloned into pcDNA3 at the HindIII and XbaI sites. Neuroigin1-EGFP, EGFP-synaptobrevin2(VAMP2), and DsRed2-synaptobrevin2(VAMP2) constructs were described by T. Dresbach. The N-cad Δ E construct was a generous gift from C. Holt (University of Cambridge, Cambridge, UK).

1. Moore R, Radice GL, Dominis M, Kemler R (1999) The generation and in vivo differentiation of murine embryonic stem cells genetically null for either N-cadherin or N- and P-cadherin. *Int J Dev Biol* 43:831–834.
2. Radice GL, et al. (1997) Developmental defects in mouse embryos lacking N-cadherin. *Dev Biol* 181:64–78.
3. Jüngling K, et al. (2006) N-cadherin transsynaptically regulates short-term plasticity at glutamatergic synapses in embryonic stem cell-derived neurons. *J Neurosci* 26:6968–6978.
4. Jüngling K, Nägler K, Pfrieger FW, Gottmann K (2003) Purification of embryonic stem cell-derived neurons by immunoisolation. *FASEB J* 17:2100–2102.
5. Mohrmann R, Lessmann V (2003) Gottmann K. Developmental maturation of synaptic vesicle cycling as a distinctive feature of central glutamatergic synapses. *Neuroscience* 117:7–18.
6. Lois C, Hong EJ, Pease S, Brown EJ, Baltimore D (2002) Germline transmission and tissue-specific expression of transgenes delivered by lentiviral vectors. *Science* 295:868–872.
7. Rubinson DA, et al. (2003) A lentivirus-based system to functionally silence genes in primary mammalian cells, stem cells and transgenic mice by RNA interference. *Nat Genet* 33:401–406.
8. Wittenmayer N, et al. (2009) Postsynaptic Neuroigin1 regulates presynaptic maturation. *Proc Natl Acad Sci USA* 106:13564–13569.

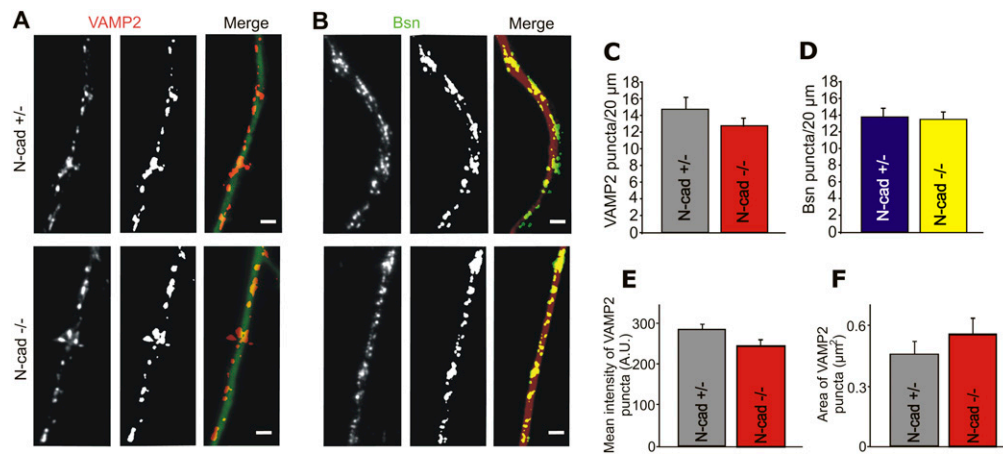


Fig. S1. Density of presynaptic vesicle clusters in mature neurons at 10–14 DIV. (A and B) Immunocytochemical stainings of vesicle clusters, Bassoon clusters, and dendrites in mouse ES cell-derived neurons at 14 DIV. (A) Neurons were costained for the synaptic vesicle protein synaptobrevin2(VAMP2) and the dendritic marker protein MAP2. (Left) Original VAMP2 staining. (Center) Thresholded VAMP2 puncta. (Right) Overlay of VAMP2 puncta (red) and MAP2 stained proximal dendrite (green). (B) Neurons were costained for the active zone protein Bassoon (Bsn) and MAP2. (Left) Original Bassoon staining. (Center) Thresholded Bassoon puncta. (Right) Overlay of Bassoon puncta (green) and MAP2 stained proximal dendrite (red). N-cad^{+/-}, control neurons; N-cad^{-/-}, homozygous N-cadherin knockout neurons. (C, E, and F) Quantification of the density (C), the mean intensity (E), and the area (F) of VAMP2 puncta on dendrites at 10–14 DIV. N-cad^{+/-}, $n = 10$; N-cad^{-/-}, $n = 14$. (D) Quantification of the density of Bassoon puncta on dendrites at 10–14 DIV. N-cad^{+/-}, $n = 13$; N-cad^{-/-}, $n = 12$. (Scale bars: 2 μm .) Mean \pm SEM.

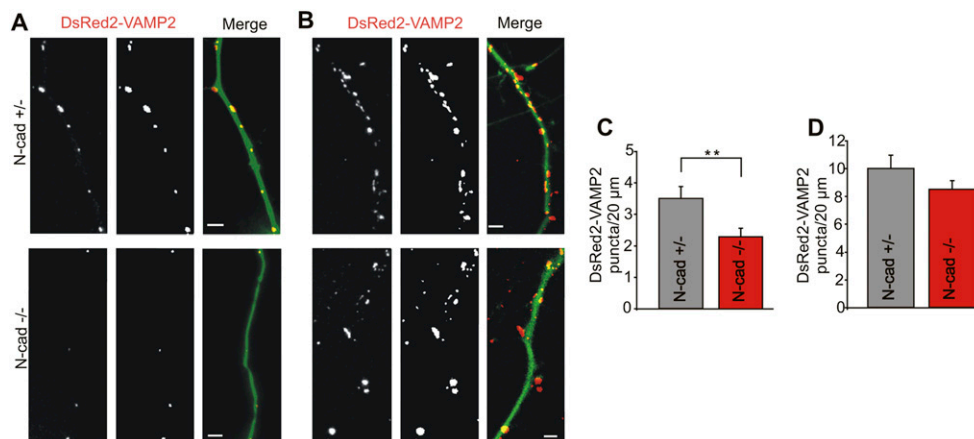


Fig. S2. The density of vesicle clusters is reduced in immature N-cadherin knockout neurons. (A and B) Fluorescence images of dendrites in ES cell-derived neurons at 7 (A) and 14 DIV (B) cotransfected with DsRed2-VAMP2(synaptobrevin2) for labeling vesicle clusters and EGFP to label dendrites by using the lipofectamine technique. (Left) Original DsRed2-VAMP2 images. (Center) Thresholded DsRed2-VAMP2 puncta. (Right) Overlay of DsRed2-VAMP2 puncta (red) and EGFP-labeled proximal dendrite. N-cad^{+/-}, control neurons; N-cad^{-/-}, homozygous N-cadherin knockout neurons. (C and D) Quantification of the density of DsRed2-VAMP2 puncta on dendrites at 6–7 DIV (C: N-cad^{+/-}, $n = 26$; N-cad^{-/-}, $n = 20$) and at 10–14 DIV (D: N-cad^{+/-}, $n = 18$; N-cad^{-/-}, $n = 20$). (Scale bars: 2 μm .) Mean \pm SEM; ** $P < 0.01$, unpaired t test.

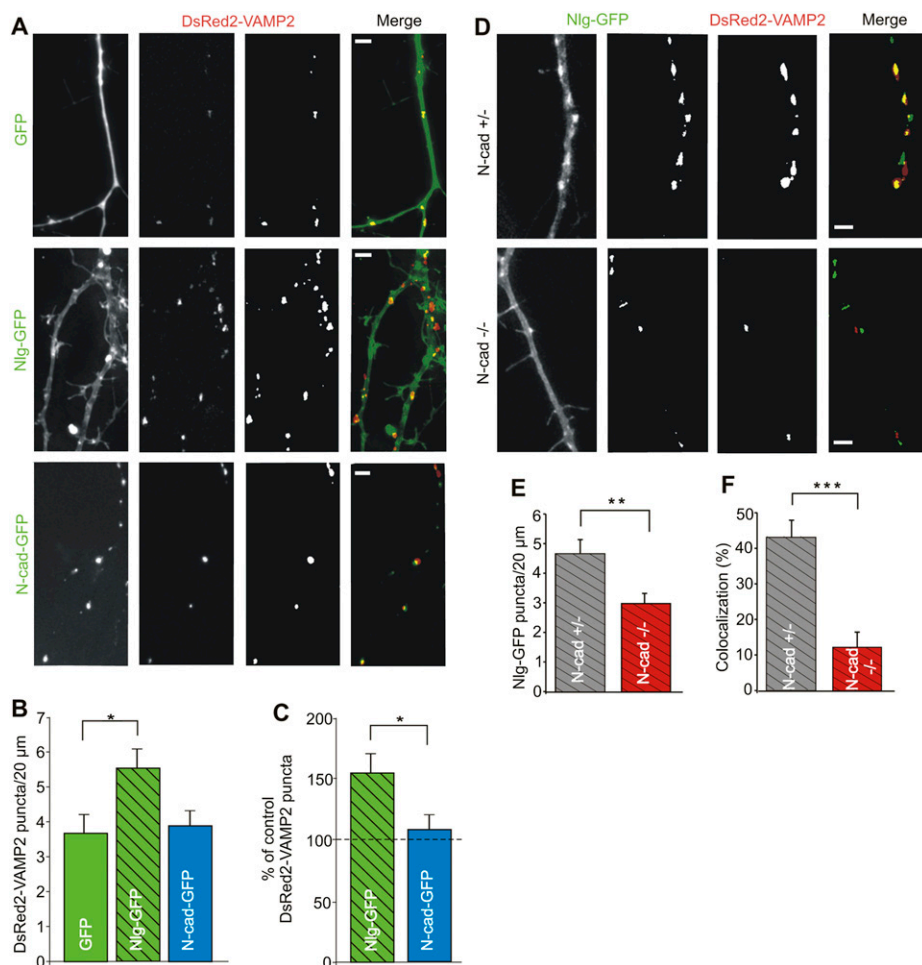


Fig. 55. Overexpression of N-cadherin fails to induce vesicle clusters, and synaptic clustering of neuroligin-1-EGFP is reduced in the absence of N-cadherin. (A–C) Expression of neuroligin-1-EGFP resulted in an increase in the density of vesicle clusters in cultured cortical neurons (6–7 DIV) as compared with EGFP expression (control). In contrast, expression of N-cadherin-EGFP did not lead to a detectable induction of vesicle clusters. DsRed2-VAMP2 (to visualize vesicle clusters) was cotransfected with either EGFP (GFP) or neuroligin-1-EGFP (Nlg-GFP) or N-cadherin-EGFP (N-cad-GFP). (A) Fluorescence images of dendrites. (Left) EGFP fluorescence to visualize dendrites. (Center) DsRed2-VAMP2 fluorescence to visualize vesicle clusters (Center Left, original images; Center Right, thresholded DsRed2-VAMP2 puncta). (Right) Overlay of EGFP fluorescence (green) and DsRed2-VAMP2 puncta (red) to visualize vesicle clusters on dendrites. (Scale bars: 2 μm.) (B and C) Quantification of the density of DsRed2-VAMP2 puncta on dendrites. Type of cotransfection is indicated on bars. GFP, $n = 24$; Nlg-GFP, $n = 27$; N-cad-GFP, $n = 16$. (D) Fluorescence images of dendrites of control (N-cad^{+/-}) and of N-cadherin knockout (N-cad^{-/-}) neurons cotransfected with neuroligin-1-EGFP and DsRed2-VAMP2. (Left) Original images of neuroligin-1-EGFP fluorescence in dendrites. (Center Left, thresholded images of neuroligin-1-EGFP puncta isolated from overall fluorescence in the dendrite. DsRed2-VAMP2, thresholded DsRed2-VAMP2 puncta visualizing presynaptic vesicle clusters. Merge, overlay of neuroligin-1-EGFP puncta (green) and DsRed2-VAMP2 puncta (red) visualizing colocalization of neuroligin-1-EGFP with presynaptic vesicle clusters. (Scale bars: 2 μm.) (E and F) Quantification of the density of neuroligin-1-EGFP puncta on dendrites (E) and quantification of colocalization of neuroligin-1-EGFP puncta with DsRed2-labeled presynaptic vesicle clusters (F). N-cad^{+/-}, $n = 31$; N-cad^{-/-}, $n = 36$ (corresponding data from the same experiments shown in Fig. 2A). Mean ± SEM; * $P < 0.05$; ** $P < 0.01$; *** $P < 0.001$, unpaired Student's t test.

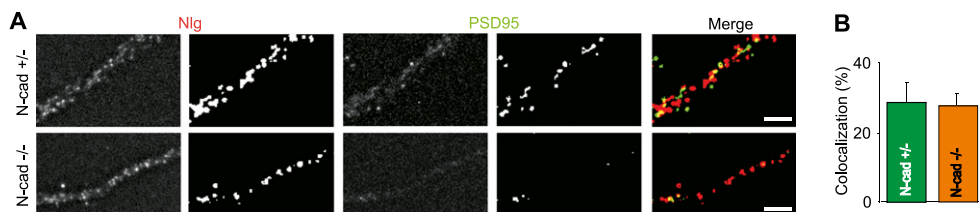


Fig. 56. Coimmunostainings of endogeneous neuroligin and PSD95 clusters in immature ES cell-derived neurons. (A) Immunocytochemical costainings of endogeneous neuroligin clusters and endogeneous PSD95 clusters in proximal dendrites of ES cell-derived neurons at 6–7 DIV. N-cad^{+/-}, control neurons; N-cad^{-/-}, homozygous N-cadherin knockout neurons. (Left) Nlg, original neuroligin staining and thresholded neuroligin puncta; (Center) PSD95, original PSD95 staining and thresholded PSD95 puncta; (Right) Merge, overlay of neuroligin puncta (red) and PSD95 puncta (green). (Scale bars: 5 μm.) (B) Quantification of the colocalization of neuroligin puncta with PSD95 puncta on dendrites (not vice versa). N-cad^{+/-}, $n = 21$; N-cad^{-/-}, $n = 21$. Mean ± SEM.

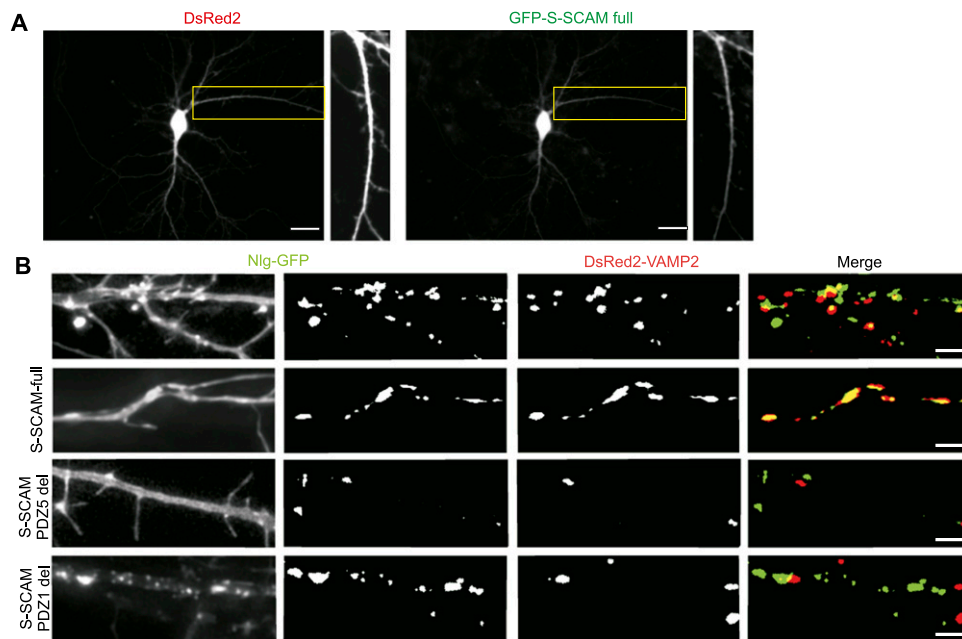


Fig. S7. Colocalization of neuroigin-1-EGFP with vesicle clusters depends on S-SCAM. (A) Expression of full-length EGFP-S-SCAM (Right) resulted in a homogeneous staining of dendrites of cultured cortical neurons (8 DIV) similar to expression of DsRed2 (Left). Insets show enlarged dendrites. (Scale bars: 10 μm .) (B) Fluorescence images of dendrites of cultured cortical neurons (6-7 DIV) cotransfected with neuroigin-1-EGFP, DsRed2-VAMP2, and either no additional vector (Top) or full-length S-SCAM (S-SCAM full), S-SCAM with PDZ5 deleted (S-SCAM PDZ5del), or S-SCAM with WW and PDZ1 deleted (S-SCAM PDZ1del). (Left) EGFP fluorescence (Nlg-GFP) visualizing neuroigin-1-EGFP puncta on dendrites (Left, original images; Center Left, neuroigin-1-EGFP puncta were isolated from overall fluorescence in the dendrite by thresholding the image). (Center Right) Thresholded DsRed2-VAMP2 puncta (vesicle clusters). (Right) Overlay of neuroigin-1-EGFP puncta (green) and DsRed2-VAMP2 puncta (red) visualizing colocalization of neuroigin-1-EGFP with vesicle clusters. (Scale bars: 2 μm .) For quantification, see Fig. 3 C-E.

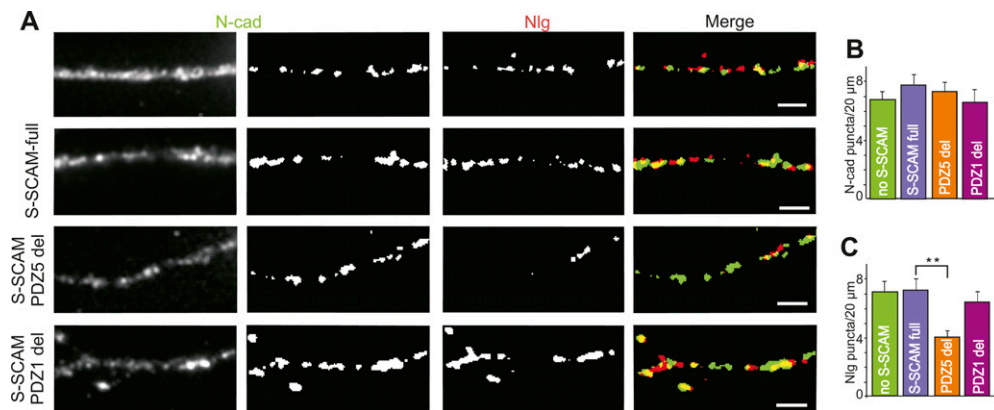


Fig. S8. Colocalization of N-cadherin and neuroigin depends on S-SCAM function. (A) Fluorescence images of dendrites of cultured cortical neurons (6-7 DIV) coimmunostained for endogeneous N-cadherin and endogeneous neuroigin, and transfected with either no additional vector (Top), full-length S-SCAM (S-SCAM full), S-SCAM with PDZ5 deleted (S-SCAM PDZ5del), or S-SCAM with WW and PDZ1 deleted (S-SCAM PDZ1del). (Left) Endogeneous N-cadherin (N-cad) (Left, original images; Center Left, N-cadherin puncta were isolated from overall fluorescence in the dendrite by thresholding the image). (Center Right) Thresholded endogeneous neuroigin (Nlg) puncta. (Right) Overlay of N-cadherin puncta (green) and neuroigin puncta (red) visualizing colocalization. (Scale bars: 2 μm .) (B and C) Quantification of the density of N-cadherin puncta on dendrites (B) and quantification of the density of neuroigin puncta on dendrites (C). Type of expressed S-SCAM is indicated. No S-SCAM, $n = 13$; S-SCAM full, $n = 11$; S-SCAM PDZ5del, $n = 12$; S-SCAM PDZ1del, $n = 13$. Mean \pm SEM; ** $P < 0.01$; one-way ANOVA. Quantification of colocalization of N-cadherin puncta with neuroigin puncta is given in Fig. 3F.

